Mon. Not. R. Astron. Soc. **328,** 977–985 (2001)

The effects of seeing on Sérsic profiles – II. The Moffat PSF

I. Trujillo,[1]★ J. A. L. Aguerri,[2] J. Cepa[1] and C. M. Gutiérrez[1]
[1]*Instituto de Astrofísica de Canarias, E-38205 La Laguna, Tenerife, Spain*
[2]*Astronomisches Institut der Universität Basel, Venusstrasse 7, CH-4102 Binningen, Switzerland*

Accepted 2001 August 21. Received 2001 August 6; in original form 2001 April 2

ABSTRACT

The effects of seeing on Sérsic $r^{1/n}$ profile parameters are extensively studied using a Moffat function. This analytical approximation to the point spread function (PSF) is shown to provide the best fit to the PSF predicted from atmospheric turbulence theory when $\beta \sim 4.765$. The Moffat PSF is additionally shown to contain the Gaussian PSF as a limiting case ($\beta \rightarrow \infty$). The Moffat function is also shown to be numerically well behaved when modelling narrow PSFs in *HST* images. Seeing effects are computed for elliptically symmetric surface brightness distributions. The widely used assumption of circular symmetry when studying the effects of seeing on intrinsically elliptical sources is shown to produce significant discrepancies with respect to the true effects of seeing on these sources. A prescription to correct raw (observed) central intensities, effective radii, index n and mean effective surface brightness is given.

Key words: atmospheric effects – methods: data analysis – galaxies: distances and redshifts – galaxies: photometry.

1 INTRODUCTION

It is well known that the ability to parametrize galaxies from ground-based images is severely compromised by seeing, which scatters light from the objects, thereby producing a loss of resolution in the images, lower mean surface brightnesses than the true values, and larger effective radii. The effects of seeing have been extensively studied in the case of elliptical galaxies with $r^{1/4}$ profiles (Franx, Illingworth & Heckman 1989; Saglia et al. 1993). Recently, Trujillo et al. (2001, hereafter T01) extended previous work by studying analytically the effects of seeing on elliptically symmetric surface brightness distributions, following the Sérsic (1968) $r^{1/n}$ law and assuming a Gaussian point spread function (PSF). Sérsic's generalization of the de Vaucouleurs (1948, 1959) $r^{1/4}$ law has been shown to provide a better representation to the distribution of light in both elliptical galaxies (including the dwarf ellipticals) and the bulges of spiral galaxies (Caon, Cappacioli & D'Onofrio 1993; D'Onofrio, Capaccioli & Caon 1994; Young & Currie 1994; Andredakis, Peletier & Balcells 1995).

The existence of 'wings' in stellar profiles reveals that the real PSF deviates from the Gaussian form. In this paper we show, from the size of the wings present in real images (e.g. Saglia et al. 1993), that such deviations from Gaussian PSFs can result in different values for the profile parameters in the range of 10–30 per cent. The new generation of ground-based telescopes and the study of galaxies at high redshifts make these types of studies crucial in order to obtain reliable (unbiased) information from the structural analysis of these objects.

This paper presents a further, more detailed, analysis of the effects of seeing on Sérsic profiles when 'wings' are present in the PSF. For this reason we have modelled the PSF by a generalization of the Gaussian form: the Moffat function (Moffat 1969), which describes well the presence of wings. It should be noted that these kinds of studies are not only important for ground-based observations. In fact, *HST* images present their own 'narrow' PSFs (see a detailed study in Bendinelli, Zavatti & Parmeggiani 1987, and Krist 1993). The use of these steep PSFs presents numerical problems, which can be avoided by modelling the narrow PSFs with polynomials instead of exponential expressions like Gaussians. In Section 2 we summarize some general results from the use of Moffat PSFs. Section 3 describes the effects of seeing on the Sérsic profile parameters brought about by the Moffat PSF. A prescription for seeing corrections is given in Section 4.

2 GENERAL REMARKS ABOUT MOFFAT CONVOLUTION

Point spread functions can be determined observationally by studying the scattering of stellar light. Numerous papers have been devoted to this problem (e.g. Moffat 1969; King 1971; Bendinelli et al. 1990). Among the analytical approximations, the Moffat function (see equation 1) has been widely used to model the PSF (e.g. Bendinelli, Zavatti & Parmeggiani 1988a,b; Young et al. 1998); for instance, the IRAF data reduction package (Tody 1986) adopts the Moffat function as a standard PSF. In Fig. 1 we plot both

★E-mail: itc@ll.iac.es

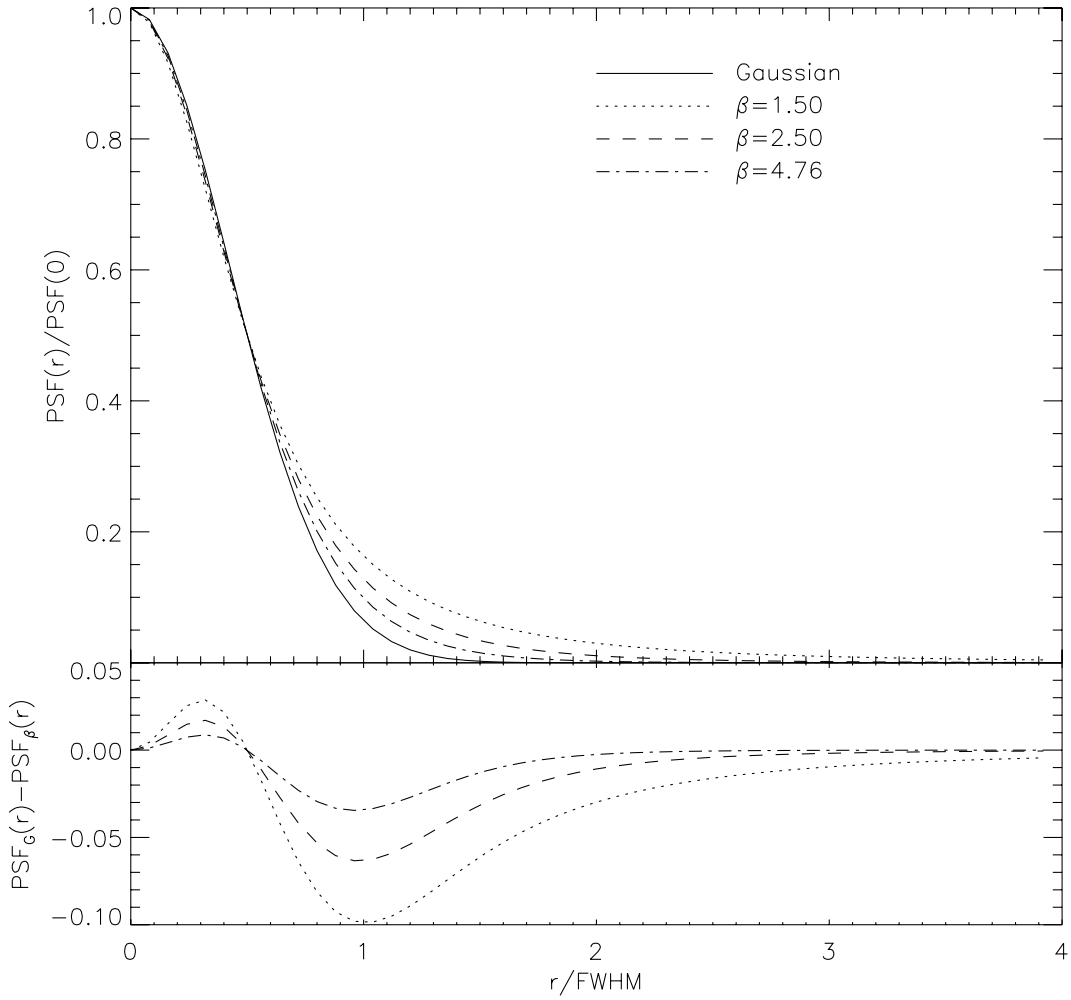

Figure 1. Top panel: The normalized intensity profile of a Gaussian function and Moffat PSF functions having different values of β are plotted against the radius of the PSF in units of FWHM. Bottom panel: The difference between the normalized Moffat PSF [$\mathrm{PSF}_\beta(r)$] and the normalized Gaussian PSF [$\mathrm{PSF}_\mathrm{G}(r$].

the Gaussian function and Moffat functions having a range of β. Note that as β increases the Moffat function tends to approximate the core of the Gaussian profile. In fact, a Moffat function contains the Gaussian PSF as a lim iting case (see Appendix A). Moreover, the Moffat PSF has two clear advantages over the Gaussian PSF:

(i) it is numerically well behaved in the treatment of narrow PSFs, and

(ii) it allows the 'wings' that usually appear in stellar profiles to be fitted.

Very accurate convolutions between the PSF and the model profiles of the galaxies are required in order to obtain reliable results. Current reduction packages use Fast Fourier Transforms to evaluate the convolutions. This is, in fact, inappropriate where there are strong changes in the intensity gradients of the galaxy profiles. The inner parts of galaxy profiles are steep, and this demands a very accurate measurement of the high frequencies in the Fourier domain. Narrow PSFs (such as those of the *HST*) magnify this problem, because they also present a steeper profile. Working in the *real* domain does not exempt us from trouble either; in fact, one can encounter several numerical problems when performing accurate convolutions using a Gaussian to model narrow PSFs. Current computers can manage numbers of the order of $\sim \mathrm{e}^{200}$. These kinds of numbers can be easily obtained when working with Gaussians which have $\sigma < 1$ in units of pixels (see the exponential expressions at play when performing a Gaussian convolution in equation 4 in T01). The use of Moffat functions avoids this problem due to the use of polynomials instead of exponential expressions (see equation 3). In this sense, Moffat functions are numerically better behaved than Gaussians when dealing with narrow PSFs.

2.1 Mathematical analysis

We will use a circular Moffat function to model the point spread function:

$$\mathrm{PSF}(r) = \frac{\beta - 1}{\pi \alpha^2}\left[1 + \left(\frac{r}{\alpha}\right)^2\right]^{-\beta}, \tag{1}$$

with the full-width at half-maximum, $\mathrm{FWHM} = 2\alpha\sqrt{2^{1/\beta} - 1}$, where $\mathrm{PSF(FWHM/2)} = (1/2)\mathrm{PSF}(0)$, and the total flux is normalized to 1. Consider a case where, in the absence of seeing, the surfaces brightness distribution, $I(\boldsymbol{r})$, of a galaxy is elliptically symmetric. This means that the isophotes of the object all have the same constant ellipticity ϵ ($\epsilon = 1 - b/a$, where a and b are respectively the semimajor and semiminor axes of the isophotes).

As shown in T01, elliptical coordinates (ξ, θ) are the most appropriate for this type of problem. In this coordinate system, the

surface brightness distribution, $I(\boldsymbol{r})$, of an elliptical source depends only on ξ: $I(\boldsymbol{r}) = I(\xi)$. The convolution equation that represents the effect of seeing on the surface brightness distribution is given by

$$I_{\rm c}(\xi,\theta) = (1-\epsilon)\int_0^\infty \xi' I(\xi')\,{\rm d}\xi' \int_0^{2\pi} {\rm d}\theta'\,{\rm PSF}(\xi',\theta',\xi,\theta), \tag{2}$$

where PSF $(\xi',\ \theta',\ \xi,\ \theta)$ is the Moffat PSF given by

$$\begin{aligned}{\rm PSF}(\xi',\theta',\xi,\theta) = {} & \frac{\beta-1}{\pi\alpha^2} \\ & \left[1+\frac{\xi^2+\xi'^2-2\xi\xi'\cos(\theta-\theta')+(\epsilon^2-2\epsilon)(\xi'\sin\theta'-\xi\sin\theta)^2}{\alpha^2}\right]^{-\beta}.\end{aligned} \tag{3}$$

The subscript 'c' will be used from here on to refer seeing-convolved quantities. Along the major axis of the object, $\theta = 0$, the angular integral can be solved analytically ($\epsilon > 0$) :

$$\begin{aligned}\int_0^{2\pi} {\rm d}\theta'\,{\rm PSF}(\xi',\theta',\xi,0) = {} & 2\frac{\beta-1}{\pi\alpha^2}a_\epsilon^{-\beta}\sum_{k=0}^{\infty} C_{2k}^{\beta}(w) \\ & \times\left[\frac{1}{a_\epsilon}\left(\frac{\xi'}{\alpha}\right)^2(2\epsilon-\epsilon^2)\right]^k B\left(\frac{1}{2},\frac{2k+1}{2}\right),\end{aligned} \tag{4}$$

where

$$a_\epsilon \equiv 1+\frac{\xi'^2(1-\epsilon)^2+\xi^2}{\alpha^2} \quad \text{and} \quad w \equiv \frac{1}{(2\epsilon-\epsilon^2)^{1/2}}\frac{\xi}{\alpha}\frac{1}{a_\epsilon^{1/2}}, \tag{5}$$

and $C_n^\lambda(t)$ and $B(z,w)$ are the Gegenbauer polynomials (Gradshteyn & Ryzhik 1980, p. 1029) and beta functions (Abramowitz & Stegun 1964, p. 258) respectively. A simpler expression is obtained for the convolution in the circularly symmetric case ($\epsilon = 0$) :

$$I_{\rm c}(r) = 2\frac{\beta-1}{\alpha^2}\int_0^\infty {\rm d}r' r' I(r') a_0^{-\beta} P_{\beta-1}\left[a_0^{-1}\left(1+\frac{r^2+r'^2}{\alpha^2}\right)\right], \tag{6}$$

where

$$a_0 \equiv \left[\left(1+\frac{r'^2-r^2}{\alpha^2}\right)^2+\left(\frac{2r}{\alpha}\right)^2\right]^{1/2}, \tag{7}$$

and $P_n(x)$ is the Legendre function of first class (Abramowitz & Stegun 1964, p. 332).

2.2 The effect of seeing on the central intensity

For any intensity distribution with elliptical symmetry, $I(\xi)$, the seeing convolved central intensity, $I_{\rm c}(\xi = 0)$, is such that

$$\begin{aligned}I_{\rm c}(0) = {} & 2\frac{\beta-1}{\alpha^2}(1-\epsilon)\int_0^\infty {\rm d}\xi'\,\xi' I(\xi') \\ & \times\frac{1}{(b^2-c^2)^{\beta/2}}P_{\beta-1}\left(\frac{b}{\sqrt{b^2-c^2}}\right),\end{aligned} \tag{8}$$

where

$$b \equiv 1+\frac{\xi'^2}{\alpha^2}\left[1+\frac{1}{2}(\epsilon^2-2\epsilon)\right] \quad \text{and} \quad c \equiv -\frac{\xi'^2}{2\alpha^2}(\epsilon^2-2\epsilon). \tag{9}$$

Note that the effect on the central intensity of the seeing convolved distribution is a function of the intrinsic ellipticity of the object. Basically, as ϵ increases, the spread of photons from the inner parts of the profile due to the seeing is more efficient, and consequently the central intensity decreases.

2.3 The effect of seeing on the ellipticity of the isophotes

In the absence of seeing, by construction, all isophotes of the profile have the same ellipticity, whereas the presence of seeing tends to make them circular. Using the isophote condition, $I_{\rm c}(\xi,0) = I_{\rm c}(\xi,\pi/2)$, it is possible to derive an implicit equation that gives the variation of the ellipticity with the radial distance:

$$\begin{aligned}\int_0^\infty \xi' I(\xi')\,{\rm d}\xi' \sum_{k=0}^{\infty}\left[\frac{C_{2k}^{\beta}(w)}{a_\epsilon^{\beta+k}}-(-1)^k\frac{C_{2k}^{\beta}(w^*)}{(a_\epsilon^*)^{\beta+k}}\right] \\ \times\left[(2\epsilon-\epsilon^2)\left(\frac{\xi'}{\alpha}\right)^2\right]^k B\left(\frac{1}{2},\frac{2k+1}{2}\right) = 0.\end{aligned} \tag{10}$$

For this problem, it is useful to introduce $a_\epsilon, w, a_\epsilon^*$ and w^* as functions of the Cartesian coordinates x,y:

$$a_\epsilon \equiv 1+\frac{\xi'^2(1-\epsilon)^2+x^2}{\alpha^2} \quad \text{and} \quad w \equiv \frac{1}{(2\epsilon-\epsilon^2)^{1/2}}\frac{x}{\alpha}\frac{1}{a_\epsilon^{1/2}} \tag{11}$$

and

$$\begin{aligned}a_\epsilon^* \equiv {} & 1+\frac{\xi'^2+y^2}{\alpha^2} \quad \text{and} \\ w^* \equiv {} & -{\rm i}\frac{1}{(2\epsilon-\epsilon^2)^{1/2}}\frac{y}{\alpha}\frac{1}{(a_\epsilon^*)^{1/2}}.\end{aligned} \tag{12}$$

From this implicit equation we can obtain y/x, and therefore the ellipticity of the isophotes affected by seeing using $\epsilon(x) = 1 - y/x$.

2.4 The ability of the Moffat function to match the atmospheric turbulence prediction of the PSF

The theory of atmospheric turbulence predicts the PSF to be the Fourier transform of $\exp[-(kb)^{5/3}]$ (Fried 1966; Woolf 1982), where FWHM $= 2.9207006b$, and b is a scaling parameter. In the *real* domain this PSF is written as

$${\rm PSF_T}(r) = \frac{1}{2\pi}\int_0^\infty kJ_0(kr)\,{\rm e}^{-\left(k\frac{\rm FWHM}{2.9207}\right)^{5/3}}\,{\rm d}k, \tag{13}$$

where J_0 is the standard Bessel function (Abramowitz & Stegun 1964, p. 358). For a given FWHM, we have evaluated the value of β that minimizes the difference between the prediction of the atmospheric turbulence theory and the Moffat function by minimizing the χ^2 of the fit between both PSFs. An optimum value of $\beta \sim 4.765$ was found. In Fig. 2 we have shown the difference between the PSF prediction from turbulence theory and a Moffat function for a value of $\beta = 4.765$. It can be seen that the agreement is quite good. A Moffat function could therefore be used to reliably model the turbulence prediction, although the PSFs usually measured in real images have bigger 'wings' or, equivalently, smaller values of β than those expected from the turbulence theory (e.g. Saglia et al. 1993). This is because the real seeing not only depends on atmospheric conditions but is also caused by imperfections in telescope optics.

The presence of these bigger 'wings' in real images makes Moffat functions a better choice to model the PSF than the turbulence theory prediction. As an example of this, current

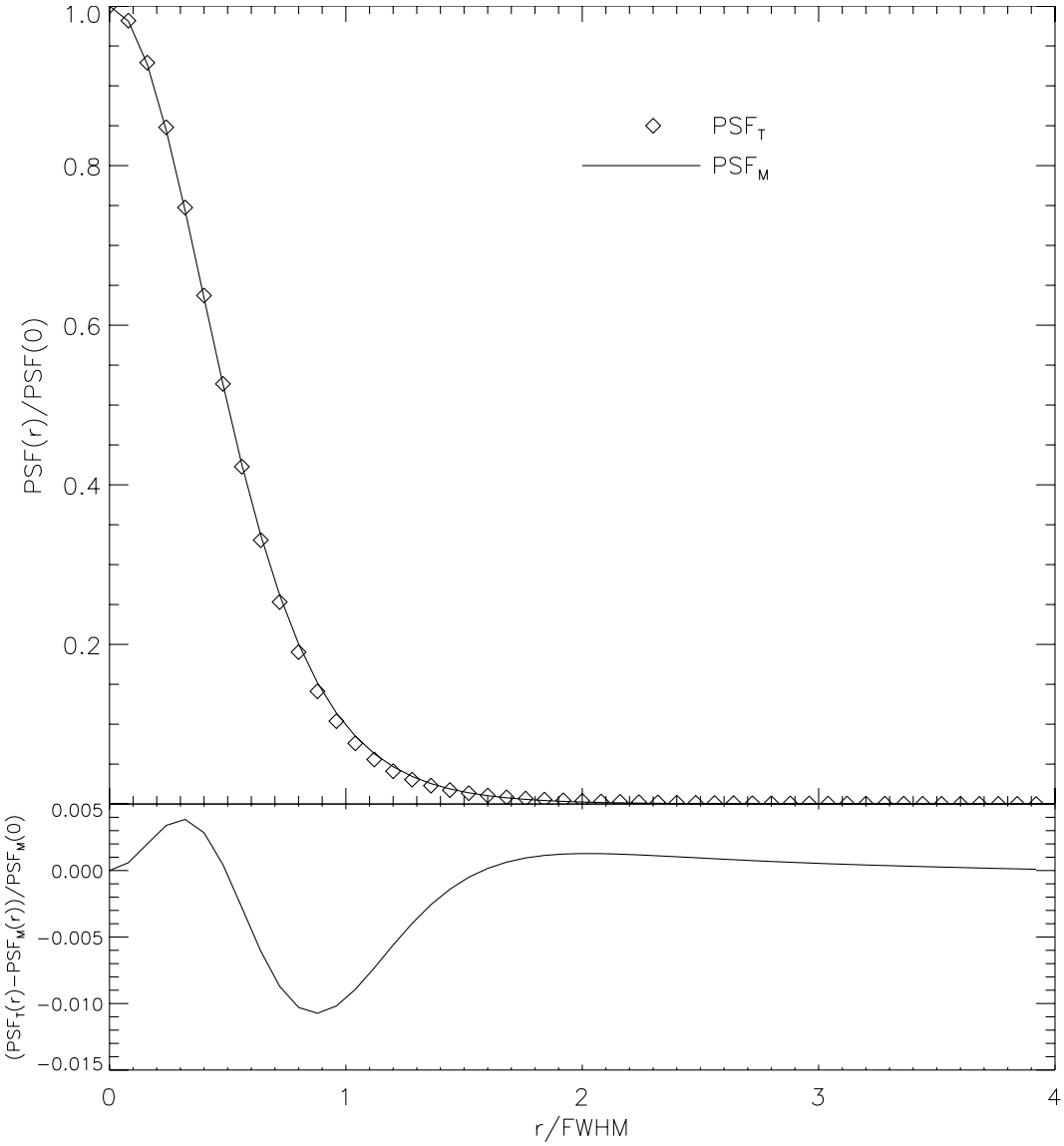

Figure 2. Top panel: The best fit to the PSF predicted by the theory of atmospheric turbulence (diamonds) using a Moffat function with a β value of 4.765 (solid line). Bottom panel: The difference between these two PSFs as a function of the radius of the PSF in unit of FWHM.

packages of data reduction in IRAF suggest a default value of $\beta = 2.5$. In order to span the range of the different 'wing' sizes present in real images, in the next section we model the Moffat PSFs using three different values of β: $\beta = 5$ (to simulate the turbulence prediction), 2.5 (the default value of the IRAF package), and 1.5 (to model a large 'wing' in the PSF).

3 THE EFFECTS OF SEEING ON THE SÉRSIC PROFILE PARAMETERS

The equations that we have shown in the previous section are general results for Moffat seeing. For practical purposes with applications to real galaxies, we are going to focus on the Sérsic profile. In the particular case of $r^{1/n}$ profiles, the surface brightness distribution is given (in elliptical coordinates) by

$$I(\xi) = I(0)10^{-b_n\left[(\xi/r_e)^{\frac{1}{n}}\right]}, \quad (14)$$

where $I(0)$ is the central intensity, and r_e the effective radius of the profile. The constant b_n is chosen such that half the total luminosity predicted by the law comes from $\xi < r_e$. b_n can be well approximated by the relation $b_n = 0.868n - 0.142$ (Caon et al. 1993).

3.1 The central intensity

To study the effect of seeing on the central intensity, we make use of equations (8) and (14). Fig. 3 shows this effect for different values of the ellipticity in the intrinsic light profile, assuming $\beta = 1.5$, 2.5 and 5, and for the Gaussian case (i.e., $\beta \rightarrow \infty$) as well.

As β increases (i.e., as the size of the PSF 'wings' decrease), we asymptotically recover the effect on the central intensity produced by a Gaussian PSF.

From this figure it follows that the effect of seeing on the central intensity increases as the size of the 'wings' increase. This is easily understood, as broader 'wings' increase the probability that a photon will hit the imaging device at a point further offset from where it would have hit in the absence of a seeing. For a typical

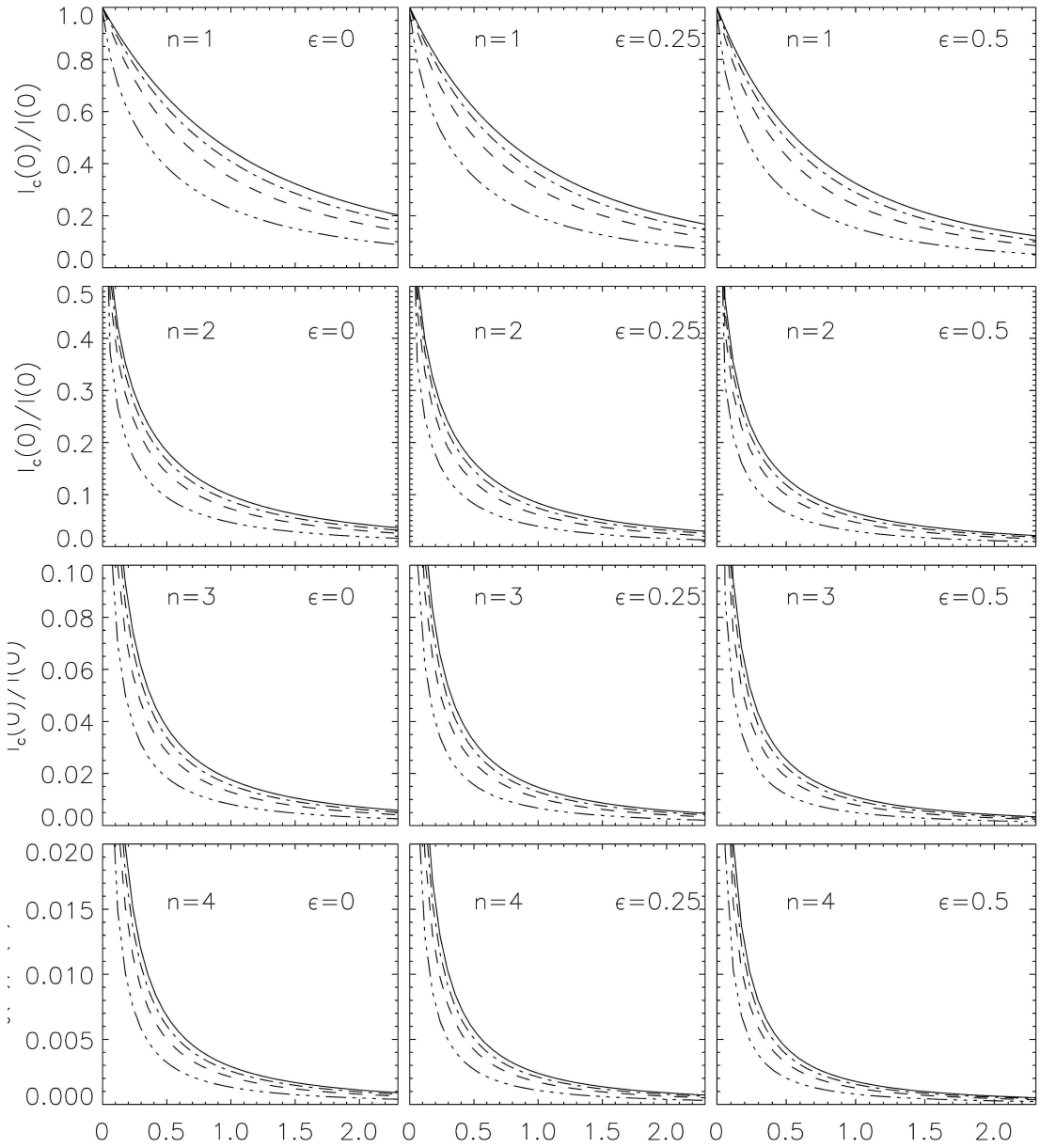

Figure 3. The effects of seeing on the observed central intensity, $I_c(0)$, for different values of n. The Gaussian case (solid line) and three different values of β are shown: $\beta = 5$ (dot-dashed line), $\beta = 2.5$ (dashed line) and $\beta = 1.5$ (dot-dot-dot-dashed line). Three different ellipticities are also shown: $\epsilon = 0$ (left column), $\epsilon = 0.25$ (middle column) and $\epsilon = 0.5$ (right column).

value of β (e.g., $\beta = 2.5$), the difference from a Gaussian PSF is ~ 10 per cent.

For a given seeing-disc (note that the relative size of the FWHM to effective radius *increases* along the x-axis of Fig. 3; cf. Figs 4 and 5), the central intensity of profiles with larger values of n is more affected than for low n, as is expected because of the higher central light concentration of these profiles. As noted in Section 2.2, the effect of seeing on the central intensity of the object is also dependent on the intrinsic ellipticity of the object: the central intensity of galaxies with larger ellipticities are more affected by seeing.

3.2 The effective radius

The seeing effect on effective radius can be obtained by solving for r_e^c from the conservation of luminosity by the convolution $L^c(r_e^c) = L(r_e)$, where $L(r_e)$ is the luminosity of the source inside r_e, and $L^c(r_e^c)$ is the luminosity obtained from the object affected by seeing, measured inside its effective radius.

Fig. 4 shows this effect for different values of ellipticity, with $\beta = 1.5$, 2.5 and 5, and for the Gaussian PSF. Here, the presence of significant 'wings' in the PSF produces an effective radius larger than what is expected from Gaussian seeing. As n increases, the *convolved* effective radius also increases. The ellipticity effect is also shown. Greater ellipticities result in greater effective radii, and these differences are more important for greater values of n. This result is as expected due to the diminution of the central intensity with larger ellipticity. For the values of β typically present in real images ($2.5 < \beta < 4$; see Saglia et al. 1993) we obtain deviations from Gaussian seeing in the range 15–30 per cent (bigger deviations are obtained for smaller values of the ratio r_e^c/FWHM).

It should be noted that our measurement of the effective radius

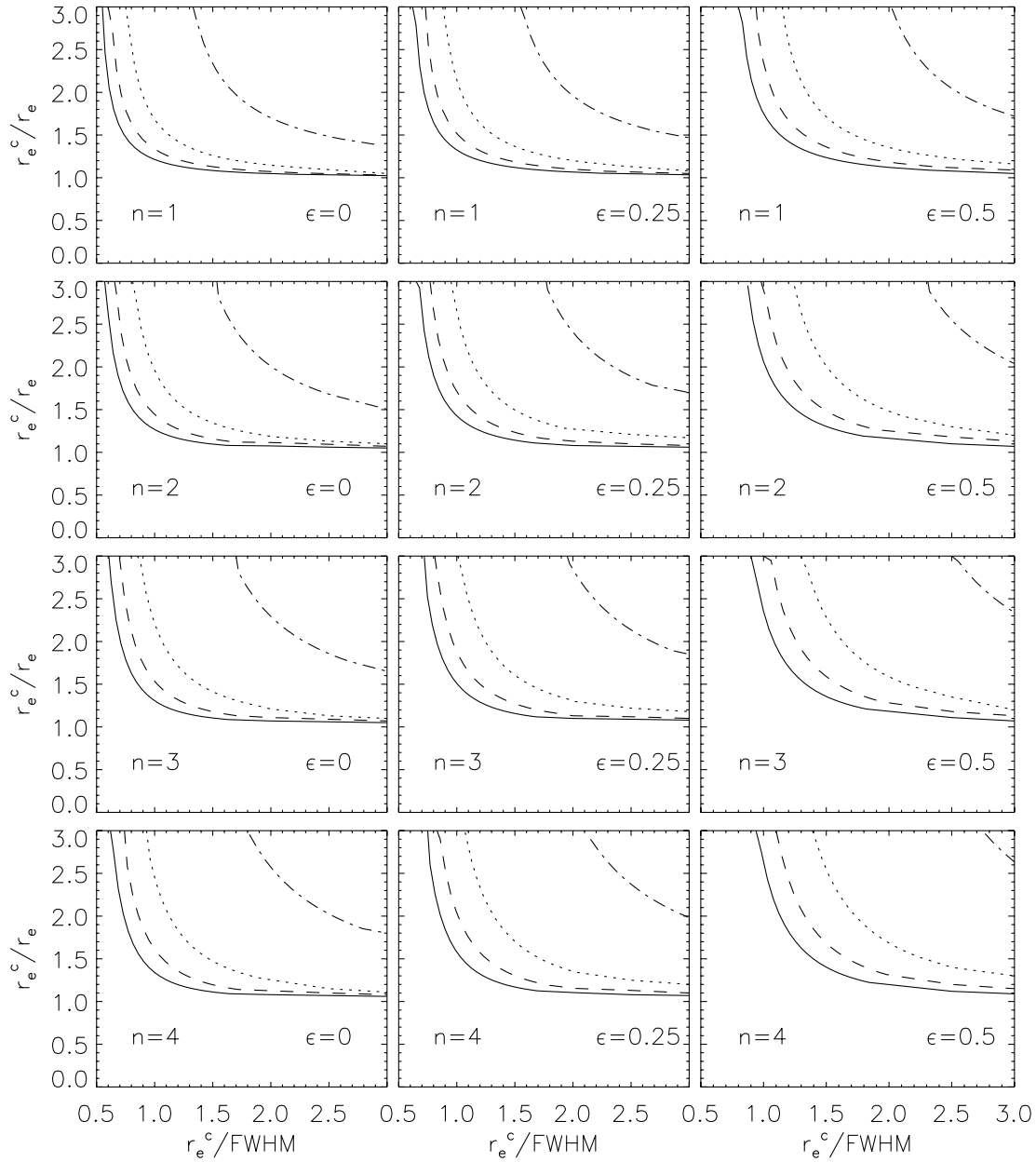

Figure 4. The effects of seeing on the observed effective radius, r_e^c for different values of n. The Gaussian case (solid line) and three different values of β are shown: $\beta = 5$ (dashed line), $\beta = 2.5$ (dotted line) and $\beta = 1.5$ (dot-dashed line). Three different ellipticities for the sources are also shown, $\epsilon = 0$ (left column), $\epsilon = 0.25$ (middle column) and $\epsilon = 0.5$ (right column).

has been obtained over the semimajor axis. Some authors use as radial distance the magnitude $r* = \sqrt{ab}$; in this case, the effective radius of the object affected by seeing is given by $r_e^{c*} = r_e^c\sqrt{1-\epsilon(r_e^c)}$, where $\epsilon(r_e^c)$ can be obtained using equation (10).

3.3 The Sérsic index *n*

To quantify the effect of seeing on the shape parameter n, we use the parameter $\eta(\xi)$ (T01). $\eta(\xi)$ is equivalent, locally, to the parameter n of the Sérsic profile. This parameter can be understood as a measure of the slope of the profile. In Fig. 5 we show the effects of seeing on this parameter (evaluated at r_e^c) for different sizes of the PSF 'wings' and different intrinsic ellipticities. It is easy to see how the real value of n is recovered asymptotically when the ratio r_e^c/FWHM increases. The effect of seeing on $\eta(r_e^c)$ is bigger for smaller values of β. This means that bigger PSF 'wings' produce a stronger effect on the slope of the profile. The increase in the intrinsic ellipticity of the profile has a similar effect, but the influence is not as important as it was for the previous parameters. Note that seeing effects always produce a surface brightness profile with a smaller value of n than the actual one. It is expected that any procedure to recover the structural parameters of the profile that does not take into account the effect of seeing will obtain lower values of n than the actual ones. Lower values of n will also be expected if the intrinsic ellipticities of the objects are not taken into account during the recovery process. This is crucial in the study of high-z galaxies. As was shown for the central intensity and effective radius, the presence of 'wings' in the PSF causes the values of the profile parameters to deviate from the prediction

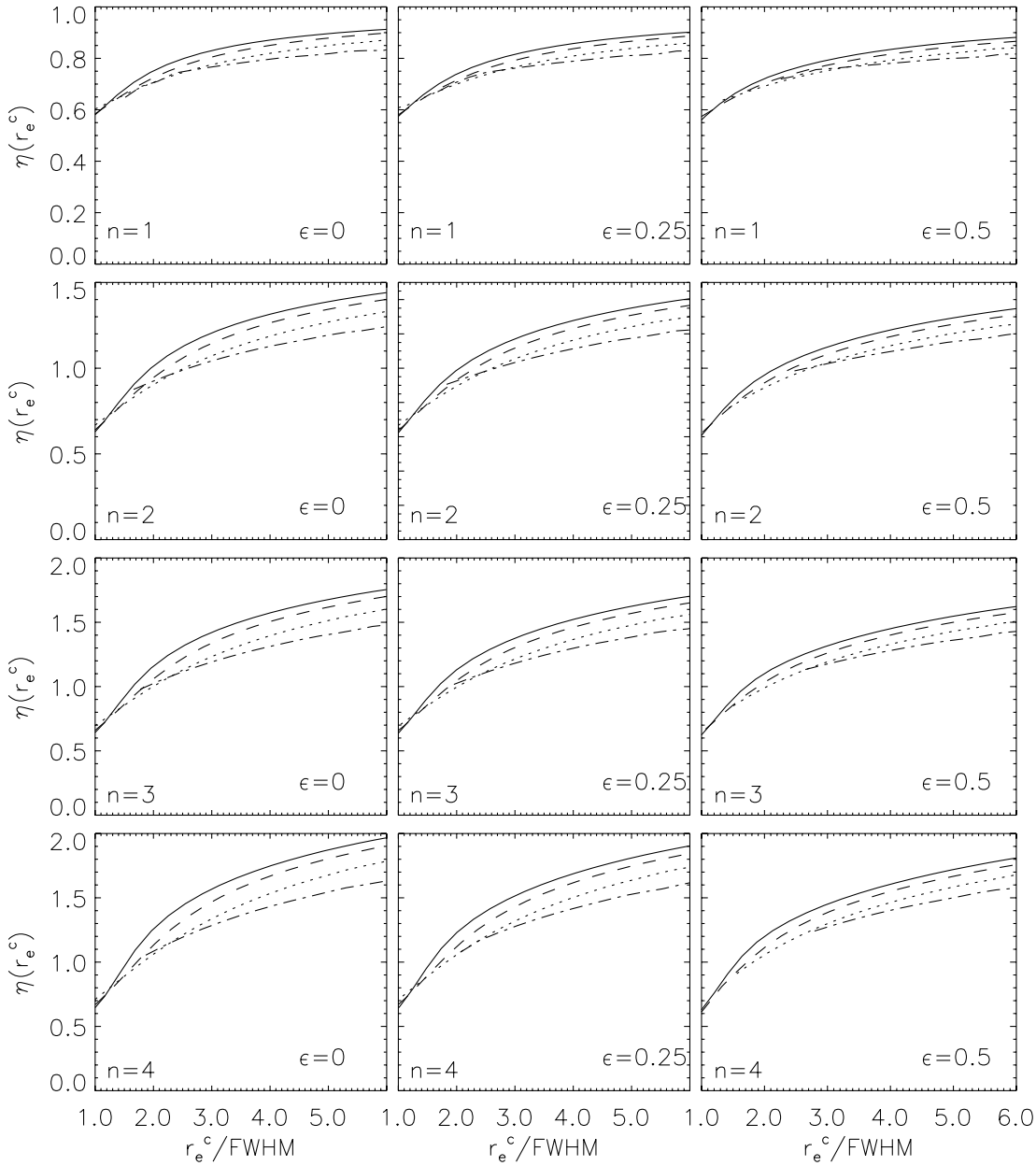

Figure 5. The effects of seeing on the index $\eta(r_{\rm e}^{\rm c})$ for different values of n. The Gaussian case (solid line) and three different values of β are shown: $\beta = 5$ (dashed line), $\beta = 2.5$ (dotted line) and $\beta = 1.5$ (dot-dashed line). Three different ellipticities for the sources are also shown, $\epsilon = 0$ (left column), $\epsilon = 0.25$ (middle column) and $\epsilon = 0.5$ (right column).

made correcting for Gaussian seeing. In the case of the $\eta(r_{\rm e}^{\rm c})$ parameter, these deviations are in the range of 10–20 per cent.

3.4 The mean effective surface brightness

From the previous results it is now easy to study the effect of seeing on the mean effective surface brightness, defined as

$$\langle\mu\rangle_{\rm e} \equiv -2.5\log\frac{L(r_{\rm e})}{\pi r_{\rm e}^2}. \tag{15}$$

By using equation (15) and the conservation of the flux, it immediately follows that

$$\Delta\langle\mu\rangle_{\rm e} \equiv \langle\mu\rangle_{\rm e}^{\rm c} - \langle\mu\rangle_{\rm e} = 5\log\frac{r_{\rm e}^{\rm c}}{r_{\rm e}}. \tag{16}$$

In Fig. 6 we show how the mean effective surface brightness changes as a function of $r_{\rm e}^{\rm c}$/FWHM for different values of n and intrinsic ellipticities. This figure clearly shows that galaxies affected by seeing have apparent mean surfaces brightnesses lower than their true values. Lower values of β produce greater effects on this quantity. Also, as the intrinsic ellipticity of the object increases, the effects of the seeing on the mean effective surface brightness also increase.

4 A PRESCRIPTION FOR SEEING CORRECTIONS

It is possible to obtain the parameters of the Sérsic profiles (seeing-free quantities) from the convolved quantities. We present an easy

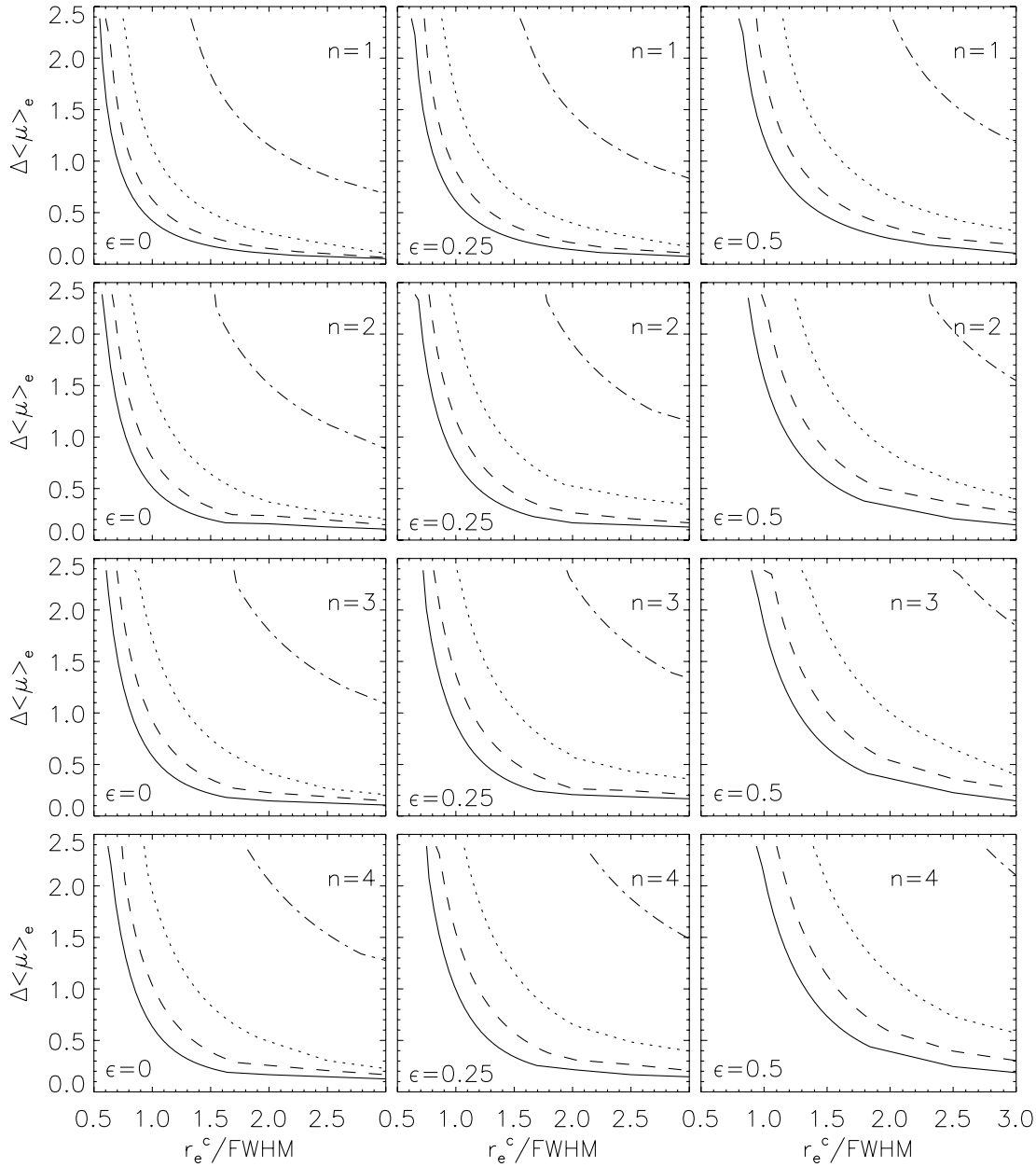

Figure 6. The differences $\Delta\langle\mu\rangle_e$ between the measured mean effective surface brightness, $\langle\mu\rangle_e^c$ and the seeing-free quantity $\langle\mu\rangle_e$ for different values of n. The Gaussian case (solid line) and three different values of β are shown: $\beta = 5$ (dashed line), $\beta = 2.5$ (dotted line) and $\beta = 1.5$ (dot-dashed line). Three different ellipticities for the sources are also shown, $\epsilon = 0$ (left column), $\epsilon = 0.25$ (middle column) and $\epsilon = 0.5$ (right column).

prescription[1] based on the use of the plots in Figs 3, 4 and 5. The steps which an observer must take are as follows.

(1) Determine the FWHM and the value of β from the stellar profile by fitting a Moffat function. Current astronomical data reduction packages, such as IRAF, allow this fitting.

(2) Measure r_e^c along the semimajor axis directly from the raw images. This can be done by solving the implicit equation $L^c(r_e^c) = (1/2)L^c(\infty)$.

(3) Determine $\eta(r_e^c)$ numerically using the expression

$$\eta(r_e^c) = \frac{1}{r_e^c}\frac{I_c(r_e^c)}{\frac{dI_c(\xi)}{d\xi}|_{r_e^c}}\ln\frac{I_c(r_e^c)}{I_c(0)}. \quad (17)$$

(4) Evaluate the value of n and ϵ from the use of Fig. 5.

(5) Obtain the value of r_e using Fig. 4.

(6) Obtain the value of $I(0)$ using Fig. 3.

5 CONCLUSIONS

As redshift increases, the apparent size of galaxies becomes progressively smaller and the effect of seeing progressively stronger. As we have seen, precise corrections for seeing are demanded in order to obtain reliable and comparable information about structural parameters from objects at the same or different redshifts. We have chosen the Moffat function to model the PSFs of real images. This choice has been made by following two criteria: the ability of this function to model the 'wings' of the PSFs present

[1] A similar prescription for Gaussian seeing is presented in T01.

in real images obtained from ground-based telescopes, and it is well behaved numerically because of its polynomial structure.

We have studied the general properties of the Moffat function when modelling PSFs. These properties can be summarized as follows: it is a very good option to model the narrow PSFs present, for example, in *HST* images because it is numerically well behaved; the Gaussian PSF is a limiting case of the Moffat PSF ($\beta \to \infty$), and the prediction for the PSF due to the theory of atmospheric turbulence can be numerically well approximated by a Moffat function with $\beta \sim 4.765$.

For practical purposes, we have analysed the effects of seeing caused by this PSF on the Sérsic model. The effects on the central intensity, effective radius, n index and mean effective surface brightness are extensively shown in Figs 3, 4, 5 and 6. We have also given an easy prescription for seeing correction that can be useful for observers in order to obtain the seeing-free quantities.

Our main results have been to show the importance of taking into account the intrinsic ellipticities of the objects and the presence of 'wings' in the PSFs for the recovery of accurate structural parameter. It is not sufficient to consider the PSF as Gaussian and assume circular symmetry to model the effects of seeing on the surface brightness distribution when the ratio of the effective radius to the FWHM is small ($\leq$2.5).

ACKNOWLEDGMENTS

We thank Alister W. Graham, who kindly proof-read versions of this manuscript.

REFERENCES

Abramowitz M., Stegun I., 1964, Handbook of Mathematical Functions. Dover, New York
Andredakis Y., Peletier R., Balcells M., 1995, MNRAS, 275, 874
Bendinelli O., Zavatti F., Parmeggiani G., 1987, JA&A, 8, 343
Bendinelli O., Zavatti F., Parmeggiani G., 1988a, Mem. Soc. Astron. Ital., 59, 547
Bendinelli O., Zavatti F., Parmeggiani G., 1988b, JA&A, 9, 17
Bendinelli O., Parmeggiani G., Zavatti F., Djorgovski S., 1990, AJ, 99, 774
Caon N., Capaccioli M., D'Onofrio M., 1993, MNRAS, 265, 1013
de Vaucouleurs G., 1948, Ann. Astrophys., 11, 247
de Vaucouleurs G., 1959, Hand. Phys., 53, 311
D'Onofrio M., Capaccioli M., Caon N., 1994, MNRAS, 271, 523
Franx M., Illingworth G., Heckman T., 1989, AJ, 98, 2
Fried D. L., 1966, J. Opt. Soc. Am., 56, 1372
Gradshteyn I. S., Ryzhik I. M., 1980, Table of Integral, Series, and Products. Academic Press, London
King I. R., 1971, PASP, 83, 199
Krist J., 1993, in Hanisch R. J., Brissenden R. J. V., Barnes J., eds, ASP Conf. Ser. Vol. 52, Astronomical Data Analysis Software and Systems II. Astron. Soc. Pac., San Francisco, p. 536
Moffat A. F. J., 1969, A&A, 3, 455
Saglia R., Bertschinger E., Baggley G., Burstein D., Colles M., Davies R., McMahan R., Wegner G., 1993, MNRAS, 264, 961
Sérsic J., 1968, Atlas de Galaxias Australes. Obs. Astronómico, Córdoba
Tody D., 1986, Proc. SPIE, 627, 733
Trujillo I., Aguerri J. A. L., Cepa J., Gutiérrez C. M., 2001, MNRAS, 321, 269, (T01)
Woolf N. J., 1982, ARA&A, 20, 367
Young C. K., Currie M. J., 1994, MNRAS, 268, L11
Young C. K., Metcalfe N., Zhu J., Wu H., Chen J. S., 1998, A&AS, 130, 173

APPENDIX A: THE GAUSSIAN AS A LIMITING CASE OF THE MOFFAT FUNCTION

The Gaussian function can be obtained from the Moffat function (MF) in the limiting case where $\beta \to \infty$. One can rewrite the MF as a function of FWHM (F) and β:

$$\mathrm{PSF}(r) = 4(2^{1/\beta} - 1)\frac{\beta - 1}{\pi F^2}\left[1 + 4(2^{1/\beta} - 1)\left(\frac{r}{F}\right)^2\right]^{-\beta}. \quad \text{(A1)}$$

As $\beta \to \infty$, we can substitute $2^{1/\beta} - 1$ with $(\ln 2)/\beta$, so

$$\lim_{\beta\to\infty}\mathrm{PSF}(r) = \lim_{\beta\to\infty}\frac{\beta - 1}{\beta}\frac{4\ln 2}{\pi F^2}\left[1 + \frac{4\ln 2}{\beta}\left(\frac{r}{F}\right)^2\right]^{-\beta}. \quad \text{(A2)}$$

Using $\lim_{m\to\infty}(1 + z/m)^m = \mathrm{e}^z$, we have

$$\lim_{\beta\to\infty}\mathrm{PSF}(r) = \frac{4\ln 2}{\pi F^2}\mathrm{e}^{-\frac{4\ln 2}{F^2}r^2}. \quad \text{(A3)}$$

Finally, writing $F^2 = 8\sigma^2 \ln 2$, we obtain

$$\lim_{\beta\to\infty}\mathrm{PSF}(r) = \frac{1}{2\pi\sigma^2}\mathrm{e}^{-\frac{1}{2}\left(\frac{r}{\sigma}\right)^2}. \quad \text{(A4)}$$

For practical purposes, a value of $\beta = 100$ is completely satisfactory for modelling a Gaussian by using a Moffat function.

This paper has been typeset from a TEX/LATEX file prepared by the author.